Modeling the Surface Structure and Stability of α-Quartz

Nora H. de Leeuw,* F. Manon Higgins, and Stephen C. Parker†

School of Chemistry, University of Bath, Claverton Down, Bath BA2 7AY, U.K.

Received: July 31, 1998; In Final Form: December 11, 1998

Atomistic simulation techniques were employed to model the {0001}, {10$\bar{1}$0}, {10$\bar{1}$1}, and {10$\bar{1}\bar{1}$} surfaces of α-quartz. The effect of associative and dissociative adsorption of water onto the surface structure is studied, and it is found that associative adsorption of water onto the {10$\bar{1}$1} surface induces the formation of Si−O−Si bridges, similar to those found on the very stable unhydrated {0001} surface. Dissociative adsorption of water is energetically favorable on all four surfaces, and hydration energies agree with experiment. Surface H^+ ions were replaced by Na^+ ions in two consecutive steps. Replacing only half the surface H^+ ions by Na^+ ions is energetically favorable, but when all H^+ ions are replaced, the surface energies and hence stabilities of the four surfaces diverge widely, which has implications for the crystal morphology. On the {10$\bar{1}\bar{1}$} surface Na−O−Na bridges are formed, which has a stabilizing effect.

Introduction

α-Quartz is one of the most abundant minerals at the earth's surface, and as such, it has been the subject of numerous studies. Experimental investigations include the synchrotron X-ray study of the growth and morphology of single crystals of natural α-quartz by Lang et al.[1] who investigated dislocations, long-range lattice properties, and surface topography. Theoretical studies include, for example, the free-energy calculations of a range of crystal properties at variable pressure and temperatures by de Boer et al.[2] and quartz amorphization.[3] In addition, the high-frequency stability of α-quartz results in its use in high-frequency devices[4,5] and in cellular and satellite network applications.[6] The need for ever smaller devices demands increased quality of single crystals of high uniformity.[4−6] Therefore, it is important to investigate any factors affecting crystal growth, for example, how reaction variables such as degree of supersaturation, temperature, solvent composition, and concentration of seed crystals influence the development of different faces of the α-quartz crystals,[7] how to minimize the number of defects and dislocations in the crystals,[8] and how pressure affects crystal growth.[9]

Water is inevitably present at crystal nucleation and growth, and when present in the bulk, it reduces the crystal strength (hydrolytic weakening),[10,11] allowing deformation of the crystal. Hence, the interaction of water with silica has been the subject of a wide range of investigations. Research into processes in the α-quartz crystal bulk have included experimental studies, such as the investigation of the role of water in controlling crack velocity in α-quartz single crystals,[12] and theoretical work, such as the LDF calculations of the hydrogarnet defect in quartz by Purton et al.[13] and ab initio calculations of $(OH)_4$ defects and interstitial water molecules in quartz.[14,15] The interstitial diffusion of water was studied along the *c*-axis in α-quartz using a CNDO self-consistent molecular orbital method[16] and along dislocation channels using a classical interatomic potential approach.[11]

However, interactions at the crystal/water interface are more pertinent to the study of crystal growth, such as the investigation of OH vibrational spectra of water molecules at quartz/water interfaces,[17] microcalorimetric measurements of the heat of interaction of water vapor with silica surfaces,[18] desorption studies,[19] and Fourier transform infrared spectra of surface hydroxyl groups.[20] However, to our knowledge, apart from the elegant work by Garofalini on water interactions with vitreous silica,[21,22] little theoretical work has been performed on the interaction of quartz surfaces with water, either physisorbed or chemisorbed. Thus, the aim of the work described in this paper is to use atomistic simulation techniques to extend our earlier work, modeling the hydroxyl groups on the {01$\bar{1}$1} surface of α-quartz described in a previous paper,[23] and to investigate the effect of dissociative and molecular adsorption of water on the surface structure and stability of a range of α-quartz surfaces. In addition to the {0001} basal plane, the surfaces considered in this paper are the {10$\bar{1}$0}, the {10$\bar{1}$1}, and its inverse the {10$\bar{1}\bar{1}$} surfaces, which are the principal faces observed in the experimental morphology.[24]

Furthermore, α-quartz crystals are routinely grown in a solution of alkali hydroxides and halides such as KOH, NaOH, and NaF.[7,9,25] Thus, we have also included in our simulations the adsorption of NaOH at different concentrations onto the various surfaces of quartz, where we aim to study the effect of the adsorption of these species on the surface structure and stability of the different crystal faces.

Theoretical Methods

The geometry and energies of adsorption of molecular and dissociated water and NaOH molecules on the quartz surfaces were modeled using atomistic simulation techniques based on the Born model of ionic solids.[26] The Born model assumes that the ions interact via long-range electrostatic forces and short-range forces, which can be described using simple analytical functions that need to be tested using, for example, electronic structure calculations. The components of the short-range forces include both the repulsions and the van der Waals attractions between neighboring electron charge clouds. The electronic polarizability of the ions is included via the shell model of Dick

* To whom correspondence should be addressed. E-mail: n.h.deleeuw@bath.ac.uk.

† E-mail: s.c.parker@bath.ac.uk.

10.1021/jp983239z CCC: $18.00
Published on Web 02/06/1999

and Overhauser[27] in which each polarizable ion, in our case the oxygen ion, is represented by a core and a massless shell connected by a spring. The polarizability of the model ion is then determined by the spring constant and the charges of core and shell. In addition, it is often necessary to include angle-dependent forces to allow for partially covalent bonds, for instance, in silica and in the water molecules.

Atomistic simulation techniques are more appropriate for this work than electronic structure calculations because of the large number of ions that need to be treated. In addition, by treating a larger portion of crystal, we can be confident that the energies are independent of crystal size. We employed static simulations to investigate the interactions between lattice ions and a full monolayer of adsorbed species to identify the strength of interaction with specific surface features. A further aim was to evaluate the energetics of both molecular and dissociative adsorption of water and NaOH at a range of different surfaces, and hence, static energy minimization techniques were chosen as the most appropriate tool.

We have modeled the quartz surfaces using the potential model for SiO_2 derived empirically by Sanders et al.,[28] which was successfully used in many previous studies, recently by us to investigate the effect of lattice relaxation on cation exchange in zeolite A.[29] The potential model for the interactions of the sodium ion with the silica framework was obtained by Post and Burnham[30] using a modified electron gas method. The potential parameters of the hydroxide ion using partial charges were those modified by Baram and Parker[23] to include a polarizable oxygen ion and were applied in their work on hydroxide formation at quartz and zeolite surfaces. The potential model for the intra- and intermolecular water interactions was successfully employed in our investigations of water adsorption on α-alumina surfaces,[31] and its derivation and further application are fully described in a previous paper of molecular dynamics simulations of hydrated MgO surfaces.[32] Although the potentials used are spherically symmetric, inclusion of the shell model means that the water molecule is represented by four centers that are deformable. The model is shown to reproduce many experimental features including coordination and hydrogen bonding distances and adsorption energies.[31] The potential parameters describing the interactions between water molecules and quartz surfaces were obtained following the approach by Schroder et al.[33] modifying the short-range Buckingham potentials as a result of the fractional charges of the water molecule's oxygen and hydrogen ions. The potential parameters used in this work are collected in Table 1.

The simulation code employed for this study was METADISE,[34] which is designed to model dislocations, interfaces, and surfaces. Following the approach of Tasker[35] the crystal consists of two blocks each comprising two regions that are periodic in two dimensions. Region I contains those atoms near the extended defect, in this case the surface layer and a few layers immediately below, and these atoms are allowed to relax to their mechanical equilibrium. Region II contains those atoms further away, which are kept fixed at their bulk equilibrium position and represent the rest of the crystal. The bulk of the crystal is simulated by the two blocks together, while the surface is represented by a single block. Both regions I and II need to be sufficiently large for the energy to converge.

The surface energy is given by

$$\gamma = \frac{U_s - U_b}{A} \tag{1}$$

where U_s is the energy of the surface block of the crystal, U_b is the energy of an equal number of atoms of the bulk crystal, and A is the surface area. The energies of the blocks are essentially the sum of the energies of interaction between all atoms. The long-range Coulombic interactions are calculated using the Parry technique,[36,37] whereas the short-range repulsions and van der Waals attraction are described by parametrized analytical expressions, such as a Buckingham potential. The surface energy is a measure of the thermodynamic stability of the surface with a low, positive value indicating a stable surface. The surface energies were calculated with respect to liquid water in order to assess the stability of the surface in an aqueous environment:

$$\gamma = \frac{E_d - (E_b + E_{H_2O})}{A} \tag{2}$$

where E_d is the energy of the surface block suitably hydrated, E_b is again the energy of the same number of bulk ions, and E_{H_2O} is the energy of bulk water. In the case of associatively adsorbed water, E_{H_2O} is the sum of the self-energy of water, calculated to be -878.0 kJ mol^{-1} using this potential model (Table 1), and the energy of condensation, obtained from a molecular dynamics simulation study[32] to be -43.0 kJ mol^{-1}, which agreed with the experimental value of -43.4 kJ mol^{-1}.[38] Thus, the energy of the reaction is simply equivalent to the energy of cleaving the crystal and adding water to the surface.

TABLE 1: Potential Parameters Used in This Work

ions	charges (e) core	charges (e) shell	core−shell interaction (eV Å^{-2})
Si	4.00000+		
H	0.40000+		
oxide oxygen	0.84819+	2.84819−	74.92038
hydroxide oxygen	0.90000+	2.30000−	74.92038
water oxygen	1.25000+	2.05000−	209.449602

Buckingham potential	A (eV)	ρ (Å)	C (eVÅ^6)
$Si^{4+}-O^{2-}$	1283.90734	0.32052	10.66158
$Si^{4+}-O^{1.4-}$	983.55600	0.32052	10.66158
$Si^{4+}-O^{0.8-}$	562.03200	0.32052	10.66158
$O^{2-}-O^{2-}$	22764.3	0.14900	27.88
$O^{2-}-O^{1.4-}$	22764.3	0.14900	13.94
$O^{1.4-}-O^{1.4-}$	22764.3	0.14900	6.97
$O^{2-}-O^{0.8-}$	22764.3	0.14900	28.92
$O^{1.4-}-O^{0.8-}$	22764.3	0.14900	8.12
$H^{0.4+}-O^{2-}$	311.97	0.25000	0
$H^{0.4+}-O^{1.4-}$	311.97	0.25000	0
$H^{0.4+}-O^{0.8-}$	396.27	0.2500	10.0

Lennard-Jones potential	A (eVÅ^{12})	B (eVÅ^6)
$O^{0.8-}-O^{0.8-}$	39344.98	42.15

Morse potential	D (eV)	α (Å$^{-1)}$	$r_{0\,(}$Å)
$H^{0.4+}-O^{1.4-}$	7.052500	3.17490	0.94285
$H^{0.4+}-O^{0.8-}$	6.203713	2.22003	0.92376

three-body potential	k (eV rad^{-2})	Θ_0
$H^{0.4+}-O^{0.8-}{}_{shell}-H^{0.4+}$	4.19978	108.693195
$O^{2-}-Si^{4+}-O^{2-}$	2.09724	109.470000
$O^{1.4-}-Si^{4+}-O^{1.4-}$	2.09724	109.470000
$O^{2-}-Si^{4+}-O^{1.4-}$	2.09724	109.470000

Coulombic subtraction	(%)
$H^{0.4+}-O^{0.8-}$	50
$H^{0.4+}-H^{0.4+}$	50

TABLE 2: Lattice Energies of α-Quartz and $Si(OH)_4$

	lattice energy/kJ mol^{-1}
$SiO_{2(s)}$	−12414.0
$Si(OH)_{4(g)}$	−10784.6

The adsorption energies were calculated with respect to gaseous water as well as liquid water to facilitate direct comparison with energies obtainable by experimental techniques such as temperature-programmed desorption and microcalorimetric measurements. The calculation of the surface and adsorption energies of dissociative adsorption of water and NaOH required a value for the energy of dissociation of a water molecule:

$$H_2O_{(g)} + O^{2-}_{(g)} \rightarrow 2OH^-_{(g)} \quad (3)$$

However, this requires the second electron affinity of oxygen, which is material-dependent.[39] This can be overcome by using experimental heats of formation for the reaction

$$SiO_{2(s)} + 2H_2O_{(g)} \rightarrow Si(OH)_{4(g)} \quad (4)$$

The reaction enthalpy for reaction 4 was found to be 30.7 kJ mol^{-1},[40,41] and by use of that, with the calculated lattice energies given in Table 2, the energy of dissociation in reaction 3 was evaluated to be −1155.9 kJ mol^{-1}.

Results and Discussion

Quartz has a hexagonal structure with space group $P3_121$.[42] The silicon atoms are four-coordinated in a tetrahedral arrangement by oxygen atoms that form bridges between two silicons. We used a unit cell of $a = b = 4.913$ Å, $c = 5.404$ Å, $\alpha = \beta = 90°$, and $\gamma = 120°$.[42] By use of the potential model by Sanders et al.,[28] the bulk crystal was then allowed to relax to a minimum energy configuration giving $a = b = 4.8177$ Å, $c = 5.375$ Å, $\alpha = \beta = 90°$, and $\gamma = 120°$.

We modeled the dissociative and associative adsorption of water at a range of quartz surfaces that were hydrated to full monolayer coverage. The initial sites chosen for molecular adsorption of water onto the surfaces were above surface oxygen ions and silicon ions. When adsorbing onto the silicon sites, the oxygen atom of the water molecule was initially positioned above the surface silicon ion, after which the surface was allowed to relax and find the minimum energy configuration. Adsorption at the surface oxygen sites was modeled by positioning one of the water molecule's hydrogen atoms at a hydrogen bond distance of 1.8 Å (experimental value of 1.76−1.95 Å in ice).[43]

In the case of dissociative adsorption of water, a dissociated water molecule was adsorbed on every surface cation−oxygen pair and in effect every surface oxygen was replaced by two hydroxyl groups, i.e., in Kröger−Vink notation,

$$H_2O + O_O{}^x \rightarrow (OH)_O{}^\bullet + (OH)_i{}' \quad (5)$$

resulting in terminal SiOH groups at the surface as detected by Koretsky et al.[20] using diffuse reflectance infrared spectroscopy. For adsorption of NaOH onto the surfaces, the reaction process is as follows:

$$NaOH + O_O{}^x \rightarrow (ONa)_O{}^\bullet + (OH)_i{}' \quad (6)$$

or

$$NaOH + O_O{}^x \rightarrow (OH)_O{}^\bullet + (ONa)_i{}' \quad (7)$$

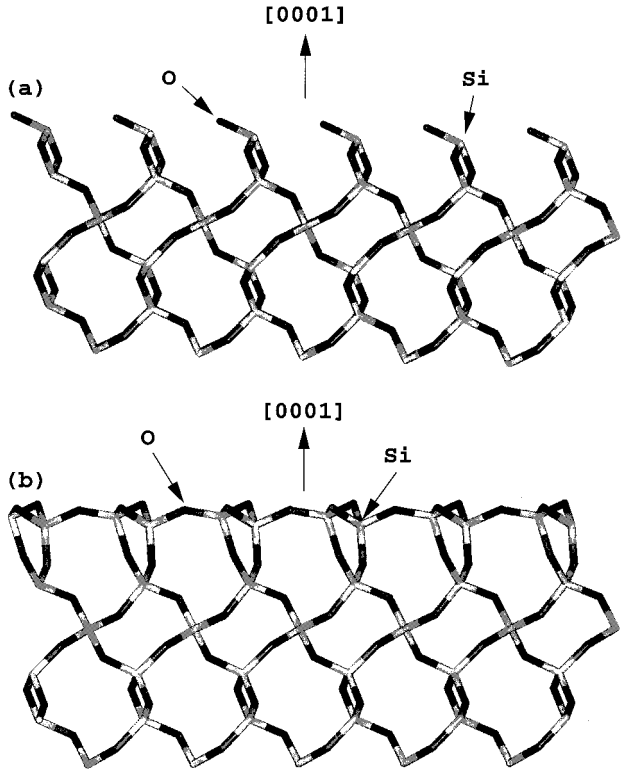

Figure 1. (a) Unrelaxed pure {0001} surface showing low-coordinated surface species and (b) relaxed surface after energy minimization, showing Si−O−Si bridges (Si = light gray, O = dark gray).

TABLE 3: Surface Energies of α-Quartz Surfaces with and without Adsorbed Species

	surface energies/J m^{-2} adsorbed species				
surface	pure	molecular H_2O	dissociated H_2O	NaOH	Na_2O
{000$\bar{1}$}	1.92	1.66	0.43	0.62	8.39
{10$\bar{1}$0}	2.77	1.89	0.39	0.72	2.69
{10$\bar{1}\bar{1}$}	2.34	1.41	0.32	1.21	1.70
{10$\bar{1}\bar{1}$}	2.48	2.22	0.37	1.22	−0.63

and

$$2NaOH + O_O{}^x \rightarrow (ONa)_O{}^\bullet + (ONa)_i{}' + H_2O \quad (8)$$

We need to be confident that in each case the most stable configuration is located; thus, many possible configurations were investigated. In the case of molecular adsorption a range of adsorption modes of the water molecules was studied and the energetically most favorable configurations were selected. All energies quoted are those of the most stable surface configurations found.

Pure Surfaces. The relaxed crystal was cut to obtain the {0001}, {10$\bar{1}$0}, {10$\bar{1}$1}, and {10$\bar{1}\bar{1}$} surfaces. The surfaces were then energy-minimized to allow for surface relaxation and to obtain their surface energies, which are given in Table 3. It is clear that the {0001} surface is, by virtue of the lowest surface energy, the most stable of the four planes. The two inverse planes, the {10$\bar{1}$1} and {10$\bar{1}\bar{1}$} surfaces, have very similar surface energies and could therefore be expected to be found to a similar extent. The stability of the {0001} surface is due to the fact that all the surface silicon atoms relax to become fully four-coordinated, forming Si−O−Si bridges on the surface (Figure 1), similar to the bulk structure. These Si−O−Si bridges have recently been observed on Si metal as well, where they

TABLE 4: Energies of Hydration of Pure and Hydroxylated α-Quartz Surfaces

	hydration energies/kJ mol^{-1}					
	molecular water on unhydrated surface		dissociated water on unhydrated surface		molecular water on hydroxylated surface	
surface	gaseous	liquid	gaseous	liquid	gaseous	liquid
{0001}	−75.8	−32.4	−227.1	−183.7	−28.0	+ 15.4
{10$\bar{1}$0}	−182.6	−139.2	−418.7	−375.3	−85.9	−42.5
{10$\bar{1}\bar{1}$}	−230.2	−186.8	−449.3	−405.9	−35.7	+ 10.6
{10$\bar{1}$1}	−95.1	−51.7	−465.4	−422.0	−89.7	−46.3

TABLE 5: Energies of Adsorption of Dilute and Concentrated NaOH at α-Quartz Surfaces

	adsorption energy/kJ mol^{-1}	
surface	NaOH	Na_2O
{0001}	−160.6	+ 799.2
{10$\bar{1}$0}	−324.1	−13.6
{10$\bar{1}\bar{1}$}	−226.6	−129.3
{10$\bar{1}$1}	−253.0	−622.5

form after initial hydration of the Si(100) surface.[44] On the other surfaces, however, there is a mixture of four- and three-coordinated surface silicon atoms while many of the surface oxygen atoms are low-coordinated as well, attached to only one silicon atom. In molecular orbital terms, these low-coordinated species have dangling-bond orbitals perpendicular to the surface that have been predicted to be unstable and a significant driving force behind surface relaxation.[45] Clearly, we expect that the unsaturated Si sites will be highly reactive and initially considered their reaction with water.

Molecular Adsorption of Water. On the {0001} surface the water molecules adsorb in a regular pattern. The oxygen atom of the water molecule adsorbs to a surface silicon atom at 1.73 Å, while one hydrogen atom coordinates at a short hydrogen bond distance of 1.64 Å to a surface oxygen atom. The other hydrogen atom points slightly away from the surface and is coordinated to two surface oxygen atoms (2.0−2.2 Å). The hydrated {0001} plane has stabilized somewhat with respect to the pure surface (Table 3). The surface energy of the unhydrated plane was particularly low compared to the other surfaces studied because of the full coordination of the surface species. This surface configuration has not changed by the molecular adsorption of water molecules, with all silicon atoms still coordinated to four lattice oxygen atoms forming O−Si−O bridges. As a result, the adsorption energy of molecular adsorption of gaseous water of −75.8 kJ mol^{-1} (Table 4) is not large, indicating that the interaction between molecular water and this surface is in the region of physisorption rather than chemisorption.

The patterns of adsorption displayed on the {10$\bar{1}$0} and {10$\bar{1}\bar{1}$} surfaces are very similar to each other. On the {10$\bar{1}$0} surface the water molecules become adsorbed to the three-coordinated surface silicon atoms at 1.53 Å. Furthermore, both hydrogen atoms coordinate to the same low-coordinated surface oxygen atom (1.62 and 1.94 Å). On the {10$\bar{1}\bar{1}$} surface (Figure 2) the $Si-O_{water}$ bond is 1.63 Å with again both hydrogen atoms bonded to the same surface oxygen (1.8−2.03 Å) while one hydrogen is also coordinated to another surface oxygen at 1.72 Å. The unsaturated surface oxygen atoms have formed Si−O−Si bridges, and all surface silicon atoms are now four-coordinated, like the {0001} surface above. As a result of this close coordination of the water molecules to the otherwise low-coordinated surface species, both surfaces have stabilized, shown by their decreased surface energies with respect to the pure surfaces. The hydration energies are considerably larger than for the {0001} surface (−182.6 and −230.2 kJ mol^{-1}),

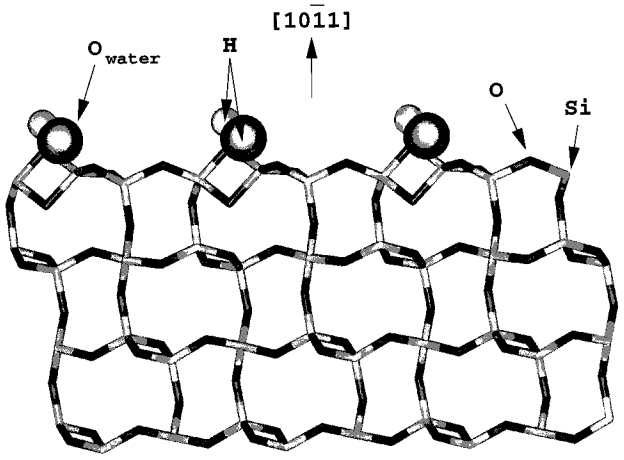

Figure 2. Relaxed {10$\bar{1}$1} surface showing Si−O−Si bridges, with associatively adsorbed water molecules (Si = light gray, O = dark gray, H = white, H_2O is shown space-filled).

indicating that on these surfaces, with unsaturated bonds, associative chemisorption takes place.

On the {10$\bar{1}\bar{1}$} surface, the water molecules again adsorb with their oxygen atoms directed toward three-coordinated surface silicon atoms but at a slightly longer distance of 1.86 Å. Both hydrogen atoms are coordinated to an unsaturated surface oxygen atom (1.6−1.68 Å), while one hydrogen also bonds to a fully coordinated surface oxygen atom at the longer distance of 2.02 Å. The larger water−silicon distance and the lesser amount of hydrogen-bonding leads to a smaller degree of stabilization than the {10$\bar{1}$0} and {10$\bar{1}\bar{1}$} surfaces above, more in the region of the {0001} surface. The adsorption energy (−95.1 kJ mol^{-1} for gaseous water) is also similar to that of the {0001} surface, more in the region of physisorption.

The mode of adsorption found at these neutral quartz surfaces, whereby the water molecule coordinates to a surface silicon atom by its oxygen atom is in agreement with experimental findings by Du et al.,[17] who used infrared−visible SFG spectroscopy to study the quartz/water interface and observed that at low pH, when the quartz surface is uncharged, the water molecules adsorb with their oxygen atoms toward the surface.

Dissociative Adsorption of Water. Dissociative adsorption at all four surfaces is energetically very favorable as is shown by the large adsorption energies and the lowering of the surface energies (Tables 3 and 4). This includes the pure relaxed {0001} surface, which has fully coordinated surface atoms and could therefore be expected to be unamenable to surface hydroxylation. Formation of SiOH species is energetically preferred, and the {0001} surface is stabilized considerably with respect to the unhydrated plane. Although the {0001} surface is amenable to dissocative adsorption by water, the stability of the planes compared to that of the pure surfaces has reversed. The {0001} suface was by far the most stable surface in its pure form, but when hydrated by dissociated water molecules, this surface has become the least stable of the series (Table 3). The {10$\bar{1}$0},

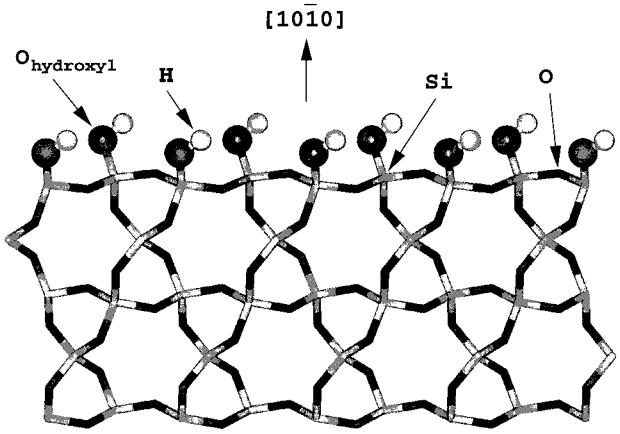

Figure 3. Relaxed {10$\bar{1}$0} surface with dissociatively adsorbed water molecules, showing proximity of the surface oxygen and hydrogen atoms (Si = light gray, O = dark gray, H = white, surface hydroxyl groups are shown space-filled).

{10$\bar{1}$1}, and {10$\bar{1}\bar{1}$} surfaces, where the surface species have dangling bonds are, as expected, highly reactive as can be seen from the large hydration energies (Table 4) and the small surface energies (Table 3). This effect of chemical reactivity increasing with decreasing coordination of the adsorbing substrate atoms was suggested by Stone[46] and confirmed in experiments,[47−49] and from previous calculations for CaO and MgO[50,51] it is a general effect.

The hydroxylated {0001} surface is the only plane containing geminal hydroxyl groups. The two geminal hydroxyl groups are not interacting with each other, but they are interacting vicinally to the neighboring group with an O−H bond length of 2.08 Å. Koretsky et al.[20] using IR spectroscopy found evidence that pointed to hydrogen-bonding either between vicinal surface groups and/or between geminal groups. We found no evidence of H-bond coordination between the geminal groups (>3 Å) and would therefore suggest that they may have found vicinal hydrogen-bonding. Vicinally interacting OH groups should be desorbed from the surface relatively easily compared to geminal and isolated hydroxyl groups,[19] which is borne out by the smaller hydration energies on this surface, where vicinal hydrogen-bonding is found extensively, compared to the other three surfaces.

Fubini et al.[18] used microcalorimetric measurements to find adsorption energies of water on powdered quartz, which can be expected to contain a wide range of surfaces, certainly the principal surfaces considered in this work. Apart from a low constant value for the adsorption energy found at high partial water pressure, energies approaching −200 kJ mol^{-1} were found at extremely low partial water pressure. Fubini et al.[18] found that the whole of the adsorbed water was easily removable by pumping at only 303 K. This easy desorption together with the much higher adsorption energies indicates the presence of vicinal and/or geminal hydroxyl groups in addition to physisorbed water but not isolated hydroxyl groups that remain on the surface even after annealing up to 873 K.[19,20] Fubini et al.'s[18] adsorption energy for geminal and/or vicinal hydroxyl groups of approximately −200 kJ mol^{-1} agrees well with the energies of dissociative adsorption found for the {0001} surface (−227 kJ mol^{-1}).

The {10$\bar{1}$0} surface also has vicinal hydroxyl groups interacting closely with each other (1.95 Å), but here there is a more extensive coordination between the hydrogen atoms and surface oxygen atoms (2.66−2.83 Å) (Figure 3). This may account for the large hydration energies, which indicate that desorption of water molecules from this surface would be difficult.

The hydroxylated {10$\bar{1}$1} and {10$\bar{1}\bar{1}$} surfaces contain isolated hydroxyl groups that do not interact with each other but are tilted by their hydrogen atoms to surface oxygen atoms (2.42−2.77 Å). Isolated hydroxyl groups are difficult to remove from quartz surfaces even at high temperatures,[19,20] which agrees with the large adsorption energies found for these surfaces.

Since dissociative adsorption of water onto the four surfaces is energetically very favorable leading to very stable surfaces and large energies of hydroxylation, it is inevitable that the surfaces will be found in hydroxylated form. As such, we were interested in investigating the effect of molecular adsorption of water onto the surface structure and stability of these hydroxylated surfaces. When water molecules were adsorbed on the surfaces, very similar adsorption patterns were observed. The water molecules form a network of hydrogen-bonding by their oxygen atom to the hydrogen atoms of the hydroxyl groups on the surface and by their hydrogen atoms to hydroxyl oxygen atoms. The hydration energies (Table 4) of molecular adsorption onto the four hydroxylated surfaces range from −90 to −28 kJ mol^{-1} for gaseous water, indicating physisorbed species as expected. Apart from the large adsorption energies found by Fubini et al.[18] at very low partial water pressure consistent with geminal and/or vicinal hydroxyl groups, at higher partial water pressures the energy leveled to a constant value of approximately −50 kJ mol^{-1}, which agrees with the range of energies of molecular adsorption on the hydroxylated surfaces described above. As stated above, Fubini et al.[18] found that all adsorbed species were easily desorbed at low temperature, which again agrees with physisorbed species in addition to the easily removed vicinal and/or geminal hydroxyl groups.

Replacement of H$^+$ by Na$^+$. We next modeled the replacement of H$^+$ by Na$^+$ on the four quartz surfaces, which is equivalent to raising the pH at high ionic strength. We modeled two Na$^+$ concentrations on the surfaces, in effect replacing either one or two H$^+$ ions by Na$^+$ ions per surface silicon atom. In the first case one Na$^+$ ion and one OH$^-$ group are added to the cleaved surface, while in the latter case one Na$^+$ ion and a NaO$^-$ group are added.

When only one sodium ion and an OH$^-$ group are adsorbed, either the sodium ion may become coordinated to a lattice oxygen or it may adsorb as a NaO$^-$ group to the silicon atom. It was found that for all surfaces the former position with the sodium ion coordinated directly to the lattice oxygen was energetically the more favorable configuration by 28 kJ mol^{-1} on the {10$\bar{1}\bar{1}$} surface to 129.5 kJ mol^{-1} on the {10$\bar{1}$0} surface.

The {0001} surface shows extensive surface relaxation. The sodium ion has become bonded to three lattice oxygen atoms (2.15−2.45 Å) and is coordinated at a longer distance (2.47 Å) to the oxygen atom of the hydroxyl group. The hydrogen is coordinated to two lattice oxygens at 2.6−2.7 Å but too distant for formal hydrogen-bonding. On the {10$\bar{1}$0} surface the sodium ion is only bonded to two lattice oxygens in addition to the hydroxyl oxygen, but at shorter distances (2.03−2.29 Å). Again, there is some remote coordination of the hydrogen to three lattice oxygen atoms (2.72−2.95 Å), and the surface has generally been smoothed with respect to the pure surface. On the two inverse surfaces {10$\bar{1}$1} and {10$\bar{1}\bar{1}$}, the sodium ion is only bonded to one previously low-coordinated lattice oxygen atom (1.94−1.96 Å) and protrudes from the planes. On the {10$\bar{1}$1} surface we find one hydrogen bond (2.17 Å), while the hydrogen atom on the {10$\bar{1}\bar{1}$} surface is more loosely coordinated to two lattice oxygen atoms at 2.47−2.58 Å.

For all four surfaces the surface energies are lowered with respect to the unhydrated surfaces but have increased, and hence the surfaces have become less stable with respect to the purely hydroxylated surfaces. The trend in surface energies and hence relative stabilities has reversed from the hydroxylated surfaces in that the {0001} surface has once more become the most stable surface even though the adsorption energy is much less than for the other surfaces. The $\{10\bar{1}0\}$ surface has a surface energy similar to that of the {0001} surface, but the adsorption energy at -324.1 kJ mol^{-1} (Table 5) is much larger because of the extensive network of strong Na−O bonding and H···O coordination. The $\{10\bar{1}1\}$ and $\{10\bar{1}\bar{1}\}$ surfaces have again very similar surface and adsorption energies because of the almost identical pattern of adsorption.

Replacement of second H^+ by Na^+. At the higher concentrations of Na^+ all of the surface hydrogen atoms are replaced by Na. This may well be the initial step to dissolution of the quartz crystal and eventual formation of Na_2SiO_3 silicate chains[52] as follows:

$$SiO_2 + 2NaOH \rightarrow Na_2SiO_3 + H_2O \qquad (9)$$

Deleuze et al.[25] proposed a reaction mechanism for reaction 9 in concentrated basic medium based on their detection of $(Si_2O_6)^{4-}{}_n$ chains in solution after dissolution of quartz in a concentrated $NaOH{\cdot}H_2O$ solution.

Although hydroxylation and adsorption of a single NaOH unit to the {0001} surface both resulted in a lowering of the surface energy and a large negative adsorption energy, replacing all H^+ by Na^+ on the surface increased the surface energy to a very high 8.39 J m^{-2} with a large positive adsorption energy of almost 800 kJ mol^{-1} (Table 5). Clearly, this is an energetically very unfavorable process, which we should not expect to take place. Structurally, the surface is disrupted for approximately 5 Å into the bulk, which may be due to the large size of the adsorbed sodium ions relative to the much smaller hydrogen atom on the hydroxylated surface. The sodium ion adsorbed as an NaO^- group is coordinated to both its own oxygen at 1.96 Å and a lattice oxygen at 2.72 Å, while the other sodium forms an O−Na−O bridge between the two geminal oxygen atoms (Na−O = 2.05 Å). The distance between the sodium ions is only 1.73 Å, and clearly, there is some degree of steric hindrance due to the cation size, also suggested by Deleuze et al.[25] in their dissolution study of quartz in concentrated basic medium, which could be the cause of the very unfavorable adsorption energy.

Although the $\{10\bar{1}0\}$ surface has not been destabilized like the {0001} surface above, the surface energy has not decreased either. Unlike hydroxylation and adsorption of the dilute NaOH on the surface, both of which stabilized the surface, adding concentrated Na_2O to the surface had no effect on the surface energy compared to the pure surface. However, it is only barely energetically favorable with an adsorption energy of -13.6 kJ mol^{-1}. On this surface, the sodium ions are not very close together (3.42 Å) and one of the sodium atoms is coordinated to three oxygen atoms (∼2.3 Å). However, the sodium atom from the NaO^- group is only bonded to its own oxygen atom (1.91 Å) and protrudes from the surface. Thus, instead of a smooth surface and some oxygen−hydrogen coordination as was the case for the adsorption of dilute NaOH, adding NaO^- to the surface results in a ruffled plane without wide-ranging surface−adsorbate interactions leading to the negligible adsorption energy.

For the first time the $\{10\bar{1}1\}$ and $\{10\bar{1}\bar{1}\}$ surfaces show radically different behavior on adsorption. On the $\{10\bar{1}1\}$ plane, one of the two types of sodium ions is again bonded to three oxygen atoms (2.33−2.45 Å) while the other one is only bonded to one previously low-coordinated oxygen (1.92 Å), similar to the $\{10\bar{1}0\}$ surface above. The distance between the two sodium ions is 2.82 Å, and there is no noticeable strain in the surface that shows bulk termination. However, while on the pure surface one low-coordinated oxygen was protruding from the surface; this has now become bonded to a sodium ion, while the NaO^- group has become coordinated to the three-coordinated silicon.

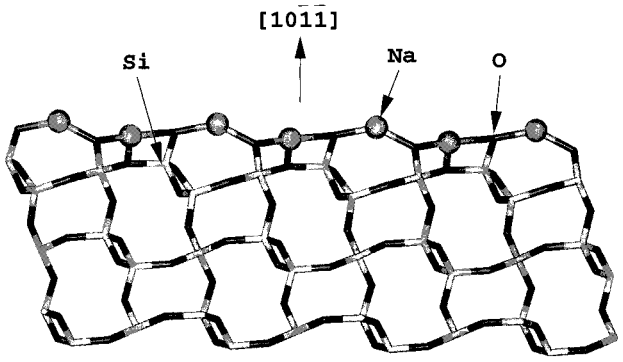

Figure 4. Relaxed $\{10\bar{1}\bar{1}\}$ surface with all H^+ ions replaced by Na^+ ions, showing surface Na−O−Na bridges (Si = light gray, O = dark gray, Na = pale gray, Na is shown space-filled).

The $\{10\bar{1}\bar{1}\}$ surface is smooth, showing bulk termination with a Na−Na distance of 3.44 Å (Figure 4). One sodium ion is again bonded to three oxygen atoms (1.92−2.27 Å), but this time the other sodium ion is coordinated to two rather than one oxygen atom (1.84 Å). An additional feature of this surface is that adsorption of the sodium ions has led to the formation of Na−O−Na bridges comparable to the Si−O−Si bridges on the very stable pure {0001} surface and in the bulk crystal.

The surface and adsorption energies of the two inverse surfaces were very similar from pure surfaces, through adsorption of dissociated water to adsorption of dilute NaOH. However, on adsorption of concentrated NaOH they show different behavior both from the {0001} and $\{10\bar{1}0\}$ surfaces and from each other. When Na^+ replaces all H^+ on the $\{10\bar{1}1\}$ surface, it is stabilized, but not as much as when either dissociated water or NaOH was adsorbed on the surface. In fact, unlike the {0001} and $\{10\bar{1}0\}$ surfaces above, both stabilization of the surface and adsorption energies have steadily decreased on the $\{10\bar{1}1\}$ surface in the adsorption series from the dissociative adsorption of water through NaOH to Na_2O, probably because of the increased cation size.

The $\{10\bar{1}\bar{1}\}$ surface, however, is stabilized to such an extent on adsorption of Na_2O that the surface energy has become negative, which means that now the surface has become more stable than the bulk, indicating that this surface will not grow but will rather dissolve, in agreement with findings of Deleuze et al.[25] who found dissolution of α-quartz to take place in concentrated NaOH solution. As expected from the negative surface energy, the adsorption energy is very large and replacing all H^+ ions with Na^+ ions is obviously a thermodynamically very favorable process, probably because of the formation of the Na−O−Na bridges leading to a smooth plane consisting of fully coordinated surface species.

Figure 5 shows a graph of the surface energy of the four surfaces versus the number of adsorbed sodium ions per surface silicon. It is clear that only at high Na concentration do the surface energies diverge sufficiently from each other to become important for crystal dissolution and to have an effect on growth of the crystal. Since the effect on surface energy is due to both the strength of interaction with the surface atoms and the steric

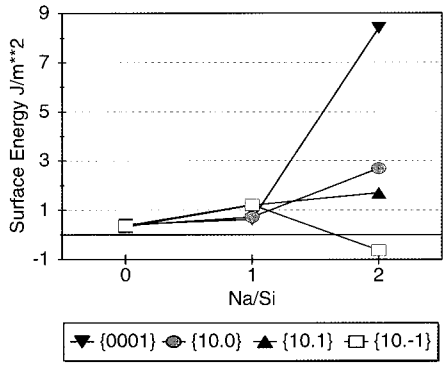

Figure 5. Graph showing the change in surface energy with number of surface H^+ ions replaced by Na^+ ions.

interaction between the adsorbed cations, Figure 5 suggests that when the solution consists of larger cations, these may have a similar effect on the surface energies at a lower concentration.

Conclusion

We have investigated the effect of molecular and dissociative adsorption of water and NaOH on the surface structure and stability of the principal experimentally observed planes of α-quartz. As a result, we can make the following observations.

The {0001} is by far the most stable of the pure surfaces because of the formation of O−Si−O bridges on the surfaces with all surface silicon and oxygen atoms becoming fully coordinated. This surface configuration is maintained on molecular adsorption of water, leading to a small hydration energy indicative of physisorption.

Molecular adsorption of water onto the other three surfaces is also energetically favorable, and the energies of adsorption vary from physisorption on the $\{10\bar{1}\bar{1}\}$ surface to associatively chemisorbed water on the $\{10\bar{1}0\}$ and $\{10\bar{1}1\}$ surfaces. The adsorption of molecular water onto the $\{10\bar{1}1\}$ surface induces the formation of O−Si−O bridges similar to those on the {0001} plane.

Chemisorption of both H_2O and NaOH onto the planes stabilizes each surface with large adsorption energies. Adsorption energies of hydroxylation of the {0001} surface, which are all geminal hydroxyl groups and hence are easily desorbed from the surface,[19] agree with enthalpies found experimentally.[18] Adsorption enthalpies found by Fubini et al.[18] in the physisorption region (about −50 kJ mol^{-1}) fall in the range of our calculated adsorption energies of molecular water onto hydroxylated surfaces (−90 to −28 kJ mol^{-1}).

In concentrated NaOH, the surface energies, and hence the stability of the surfaces, diverge widely, which could be important for manipulation of the morphology in crystal growth. The solvent concentration necessary for the surface stabilities to become sufficiently different is probably determined to an important extent by the size of the adsorbed cation, and hence, cation size and solvent concentration together may be able to "tailor-make" α-quartz crystals.

In future we would like to extend this work to include partially covering the α-quartz surfaces with dissociative water molecules in order to be able to differentiate more specifically among vicinal, geminal, and isolated hydroxyl groups on the surfaces, enabling us to compare with the experimental results of Sneh and George.[19] It would also be interesting to extend this study to include the effect of pH and the adsorption of other cations such as Li^+ and K^+ to investigate whether cation size has indeed an important effect on the surface and adsorption energies, as suggested by this work. Another area of further modeling would be molecular dynamics simulations of the quartz surfaces with NaOH dissolved in liquid water.

Acknowledgment. We acknowledge EPSRC and NERC for financial support and Molecular Simulations Inc. for the provision of InsightII.

References and Notes

(1) Lang, A. R.; Makepeace, A. P. W.; Moore, M. *Miner. Mag.* **1994**, *58*, 87.
(2) de Boer, K.; Jansen, A. P. J.; van Santen, R. A.; Watson, G. W.; Parker, S. C. *Phys. Rev. B* **1996**, *54*, 826.
(3) Watson, G. W.; Parker, S. C. *Phys. Rev. B* **1995**, *52*, 13306.
(4) Hickel, P. E.; Lafon, F.; Fortis, F.; Cambon, O.; Demazeau, G. *Ann. Chim. Sci. Mater.* **1997**, *22*, 571.
(5) Hickel, P. E.; Lafon, F.; Chvansky, P. P.; Largetreau, A.; Demazeau, G. *Ann. Chim. Sci. Mater.* **1997**, *22*, 583.
(6) Balascio, J. F.; Lind, T. *Curr. Opin. Solid State Mater. Sci.* **1997**, *2*, 588.
(7) Lee, K. J.; Seo, K. W.; Yu, H. S.; Mok, Y. I. *Korean J. Chem. Eng.* **1996**, *13*, 489.
(8) Arnaud, R.; Cambon, O. *Ann. Chim. Sci. Mater.* **1997**, *22*, 577.
(9) Lafon, F.; Demazeau, G. *J. Phys. IV* **1994**, *4C2*, 177.
(10) Griggs, D. T.; Blacic, J. D. *Science* **1965**, *147*, 292.
(11) Heggie, M. I.; Jones, R.; Latham, C. D.; Maynard, S. C. P.; Tole, P. *Philos. Mag. B* **1992**, *65*, 463.
(12) Reuschle, T.; Darot, M. *Eur. J. Mineral.* **1996**, *8*, 695.
(13) Purton, J.; Jones, R.; Heggie, M.; Oberg, S.; Catlow, C. R. A. *Phys. Chem. Miner.* **1992**, *18*, 389.
(14) Lin, J. S.; Payne, M. C.; Heine, V.; McConnell, J. D. C. *Phys. Chem. Miner.* **1994**, *21*, 150.
(15) Jones, R.; Oberg, S.; Heggie, M. I.; Tole, P. *Philos. Mag. Lett.* **1992**, *66*, 61.
(16) Hagon, J. P.; Stoneham, A. M.; Jaros, M. *Philos. Mag. B* **1987**, *55*, 225.
(17) Du, Q.; Freysz, E.; Shen, Y. R. *Phys. Rev. Lett.* **1994**, *72*, 238.
(18) Fubini, B.; Bolis, V.; Bailes, M.; Stone, F. S. *Solid State Ionics* **1989**, *32*, 258.
(19) Sneh, O.; George, S. M. *J. Phys. Chem.* **1995**, *99*, 4639.
(20) Koretsky, C. M.; Sverjensky, D. A.; Salisbury, J. W.; D'Aria, D. M. *Geochim. Cosmochim. Acta* **1997**, *61*, 2193.
(21) Blonski, S.; Garofalini, S. H. *J. Phys. Chem.* **1996**, *100*, 2201.
(22) Litton, D. A.; Garofalini, S. H. *J. Non-Cryst. Solids* **1997**, *217*, 250.
(23) Baram, P. S.; Parker, S. C. *Philos. Mag. B* **1996**, *73*, 49.
(24) Dana, E. S. *Manual of Mineralogy*; Hurlbut, C. S., Ed.; John Wiley & Sons: London, 1941.
(25) Deleuze, M.; Goiffon, A.; Ibanez, A.; Philippot, E. *J. Solid State Chem.* **1995**, *118*, 254.
(26) Born, M.; Huang, K. *Dynamical Theory of Crystal Lattices*; Oxford University Press: Oxford, 1954.
(27) Dick, B. G.; Overhauser, A. W. *Phys. Rev.* **1958**, *112*, 90.
(28) Sanders, M. J.; Leslie, M.; Catlow, C. R. A. *J. Chem. Soc., Chem. Commun.* **1984**, 1271.
(29) Higgins, F. M.; Watson, G. W.; Parker, S. C. *J. Phys. Chem. B* **1997**, *101*, 9964.
(30) Post, J. E.; Burnham, C. W. *Am. Miner.* **1986**, *71*, 142.
(31) de Leeuw, N. H.; Parker, S. C. *J. Am. Ceram. Soc.*, in press.
(32) de Leeuw, N. H.; Parker, S. C. *Phys. Rev. B* **1998**, *58*, 13901.
(33) Schroder, K. P.; Sauer, J.; Leslie, M.; Catlow, C. R. A. *Chem. Phys. Lett.* **1992**, *188*, 320.
(34) Watson, G. W.; Kelsey, E. T.; de Leeuw, N. H.; Harris, D. J.; Parker, S. C. *J. Chem. Soc., Faraday Trans.* **1996**, *92*, 433.
(35) Tasker, P. W. *Philos. Mag. A* **1979**, *39*, 119.
(36) Parry, D. E. *Surf. Sci.* **1975**, *49*, 433.
(37) Parry, D. E. *Surf. Sci.* **1976**, *54*, 195.
(38) Duan, Z.; Moller, N.; Weare, J. H. *Geochim. Cosmochim. Acta* **1995**, *59*, 3273.
(39) Harding, J. H.; Pyper, N. C. *Philos. Mag. Lett.* **1995**, *71*, 113.
(40) Greenberg, S. A. *J. Phys. Chem.* **1957**, *61*, 196.
(41) Iler, R. K. *The Chemistry of Silica; Solubility Polymerisation, Colloid and Surface Properties, and Biochemistry*; John Wiley & Sons: New York, 1979.
(42) Deer, W. A.; Howie, R. A.; Zussman, J. *An introduction to the rock-forming minerals*; Longman Group: Harlow, U.K., 1992.
(43) Kamb, B. *Water and Aqueous Solutions*; Horne, R. A., Ed.; John Wiley & Sons Inc.: New York, 1972.

(44) Stefanov, B. B.; Gurevich, A. B.; Weldon, M. K.; Raghavachari, K.; Chabal, Y. J. *Phys. Rev. B* **1998**, *81*, 3908.
(45) LaFemina, J. P.; Duke, C. B. *J. Vac. Sci. Technol. A* **1991**, *9*, 1847.
(46) Stone, F. S. *J. Solid State Chem.* **1975**, *12*, 271.
(47) Jones, C. F.; Reeve, R. A.; Rigg, R.; Segall, R. L.; Smart, St. C.; Turner, P. S. *J. Chem. Soc., Faraday Trans. 1* **1984**, *80*, 2609.
(48) Onishi, H.; Egawa, C.; Aruga, T.; Iwasawa, Y. *Surf. Sci.* **1987**, *191*, 479.
(49) Ito, T.; Tashireo, T.; Kawasaki, M.; Watanabe, T.; Toi, K.; Kobayashi, H. *J. Phys. Chem.* **1991**, *95*, 4476.
(50) de Leeuw, N. H.; Watson, G. W.; Parker, S. C. *J. Phys. Chem.* **1995**, *99*, 17219.
(51) de Leeuw, N. H.; Watson, G. W.; Parker, S. C. *J. Chem. Soc., Faraday Trans.* **1996**, *92*, 2081.
(52) Guerin, M *Chim. Dunod (Paris)* **1969**.